

Evolution of Topological Order in Xe Films on a Quasicrystal Surface

Stefano Curtarolo,^{1,*} Wahyu Setyawan,¹ Nicola Ferralis,² Renee D. Diehl,² and Milton W. Cole²

¹*Department of Mechanical Engineering and Materials Science, Duke University, Durham, North Carolina 27708, USA*

²*Department of Physics and Materials Research Institute, Penn State University, University Park, Pennsylvania 16801, USA*

(Received 17 February 2005; published 21 September 2005)

We report results of the first computer simulation studies of a physically adsorbed gas on a quasicrystal-line surface Xe on decagonal Al-Ni-Co. The grand canonical Monte Carlo method is employed, using a semiempirical gas-surface interaction, based on conventional combining rules, and the usual Lennard-Jones Xe-Xe interaction. The resulting adsorption isotherms and calculated structures are consistent with the results of LEED experimental data. The evolution of the bulk film begins in the second layer, while the low coverage behavior is epitaxial. This transition from epitaxial fivefold to bulklike sixfold ordering is temperature dependent, occurring earlier (at lower coverage) for the higher temperatures.

DOI: 10.1103/PhysRevLett.95.136104

PACS numbers: 68.43.-h, 61.44.Br, 68.55.Ac

The observed unusual electronic [1,2] and frictional [3–5] properties of quasicrystal surfaces stimulate interesting fundamental questions about how these and other physical properties are altered by quasiperiodicity. Recent progress in the characterization and preparation of quasicrystal surfaces raises new possibilities for their use as substrates in the growth of films having novel structural, electronic, dynamic, and mechanical properties [6–8]. The physical behavior of systems involving competing interactions in adsorption is a subject of continuing interest and is particularly relevant to the growth of thin films [9]. Several different growth modes have been observed for the growth of metal films on quasicrystals [10–13]. The wide range of behavior observed so far indicates that, even in the absence of intermixing, film growth is strongly affected by chemical interactions between adsorbate and substrate. In order to separate these chemical effects from those specific to quasiperiodic order, we have studied the adsorption of rare gases on a quasicrystal surface, where both the gas-gas and gas-surface interactions are believed to be simple; i.e., appreciable chemical interactions and adsorbate-induced surface reconstructions are absent.

In the present work, we explore the implications of structural mismatch by evaluating the nature of Xe adsorption on a quasicrystal substrate, namely, the tenfold surface of decagonal Al-Ni-Co. This study of thermal and structural properties employs grand canonical Monte Carlo (GCMC) simulations, with which we have extensive experience [14,15]. The calculations employ the same potential function we used earlier to compute the low coverage adsorption with the virial expansion [16]. Using the GCMC method, we compute the film properties for specified thermodynamic conditions. A hard wall at 10 nm above the surface is used to confine the coexisting vapor phase. We take a square section of the surface A , of side 5.12 nm, to be the unit cell in the simulation, for which we assume periodic boundary conditions. This approach sacrifices accuracy of the long range QC structure. However, such a simplification is numerically useful for these simulations. Since the cell is large relative to the Xe size it is

accurately representative of order on short-to-moderate length scales. The simulation results, presented below, are remarkably consistent with both the results from the virial calculations [16] and with our experiment [17]: a monolayer film is found, the ordering of which reflects many aspects of the underlying structure.

The Xe-surface potential used here, shown in Fig. 1, is based on a summation of two-body interactions between the Xe and the individual constituent atoms of the substrate: Al, Ni, and Co [16]. The gas-gas potential is taken to be a Lennard-Jones (LJ) interaction, with parameter values for Xe: $\epsilon = 221$ K and $\sigma = 0.41$ nm. The Xe-substrate pair interactions are also assumed to have LJ form, with parameter values taken from traditional combining rules, using atomic sizes derived from bulk crystalline lattice constants [16–18]. In the calculation of the adsorption potential, we assumed a structure of the virgin surface taken from an empirical fit to LEED data [19].

The Xe adsorption potential derived with this procedure is both deep and highly corrugated. Depending on the lateral position (x, y) across the surface, the maximum depth as a function of normal coordinate (z) is typically

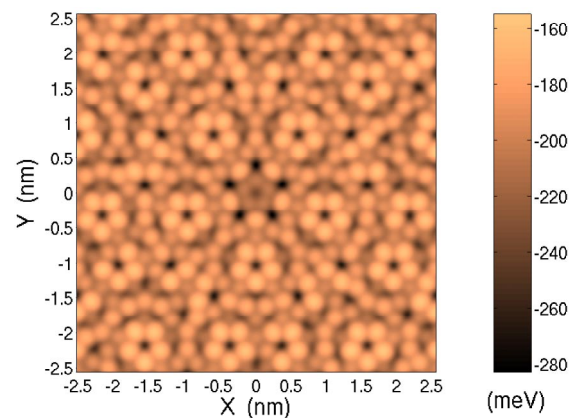


FIG. 1 (color online). Computed potential energy for Xe on Al-Ni-Co and potential energy scale (right), obtained by minimizing $V(z, y, z)$ with respect to z variation.

in the range $D(x, y) \sim 150$ to 250 meV. This potential is called “deep” because the record maximum well depth for Xe on a periodic surface is about 160 meV, viz., on graphite [20]; the record minimum well depth is about 28 meV, on Cs [21]. While the term “corrugation” is not well-defined for a nonperiodic surface, one estimate of its magnitude comes from the standard deviation of the laterally varying well depth, which is about 50 meV on this surface. Thus the well depth’s fluctuation is about 25% of its average magnitude, which is sufficiently large as to warrant the description “highly corrugated.” Using this potential, we computed the adsorption properties at low vapor pressure, P , using the virial expansion (including the first three terms). The results of that analysis were found to be semi-quantitatively consistent with our experimental data in the low coverage regime [16].

Figure 2(a) shows adsorption isotherms computed with the GCMC simulations. The temperature range extends from 70 K to 286 K (the triple temperature of Xe is 161.4 K). The plotted quantity is the thermodynamic excess coverage, N_x/A , defined as the difference between the total number of atoms in the simulation cell, and the number that would be present if the cell were filled with uniform vapor at the specified values of P and T . Detailed inspection of the isotherms reveals that there is continuous film growth (i.e., complete wetting) for all temperatures above the triple point. This behavior persists to some temperature below the triple temperature but we have not clearly established where the wetting transition occurs. At 77 K, at least 5 layers form before the onset of bulk condensation. The inset in Fig. 2(a) shows the density profile, $\rho(z)$, in the direction perpendicular to the surface, for a total surface coverage of 26.28 atoms/nm², corresponding to point “e” on the 77 K isotherm. One observes

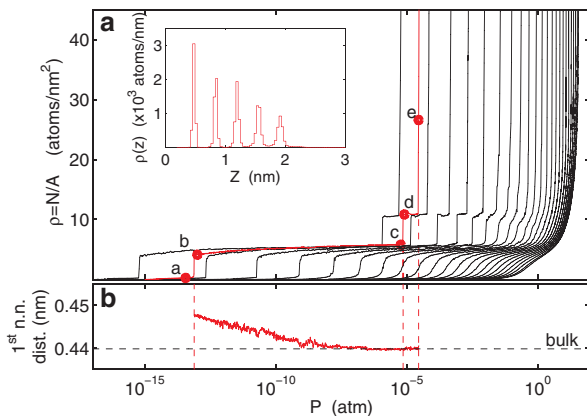


FIG. 2 (color online). (a) Computed isotherms from 70 to 286 K in steps of 10 K. Two additional isotherms at 77 and 286 K are shown. The isotherm with solid circles is for 77 K, while the highest-temperature isotherm is for 286 K. The inset shows the density profile $\rho(z)$ for $P = 0.259 \times 10^{-4}$ atm and 77 K, indicated by point “e”. (b) The nearest-neighbor distance within the first layer at 77 K approaches the condensation bulk value.

that the (perpendicular) layer structure is well-defined, in spite of the large lateral variation of the potential. Figure 2(b) shows the nearest-neighbor distance within the first layer at 77 K. This distance approaches the condensation bulk value, suggesting that only reordering within the first layer is required to effect the five to sixfold transition. Thus, the transition is continuous and happens during the completion of the first layer, between points “b” and “c” of Fig. 2(a).

Figure 3 shows the density variations within the top layer for several points on the 77 K isotherm as specified in Fig. 2(a). An animation exhibiting the film’s evolution, based on a larger set of density profiles, can be seen online [22]. At the lowest pressure (point “a”), one observes a film that has atoms localized in the deepest parts of the potential, and the Fourier transform (FT) of that density function is tenfold symmetric, reflecting the substrate symmetry. At the top of the first-layer step of the isotherm (point “b”), the density variation is more uniform, now having points of localized fivefold and sixfold symmetry. The FT of this structure is still tenfold, i.e., still reflecting the substrate symmetry. By the time the adsorption proceeds to point “c”, however, the layer has more points of local sixfold symmetry, and the FT displays sixfold symmetry. When the full bilayer has formed (point “d”) the in-

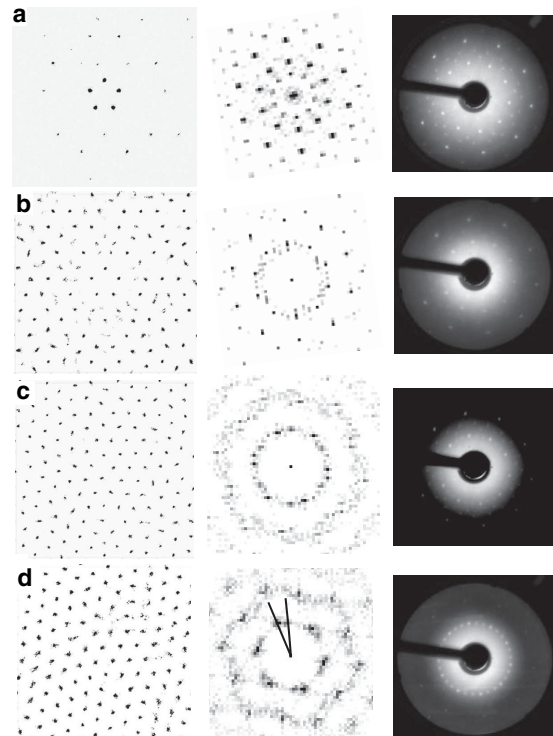


FIG. 3. Intralayer density plots for adsorption at 77 K, Fourier transforms of these plots, and LEED patterns corresponding to similar conditions. The plots show the density in the top layer, corresponding to the points noted in Fig. 2(a). The lines on the FT in panel (d) indicate the two different rotational alignments discussed in the text. Panel labels (a), (b), (c), (d) correspond to the labeled points on the isotherm in Fig. 2.

plane symmetry is clearly sixfold locally, with some dislocation defects, and the FT indicates an overall sixfold symmetry of the structure. When the sixfold structure forms, it is aligned so that the close-packed direction of the Xe is parallel to a principal fivefold direction of the substrate surface. For any given simulation run, the selection of fivefold or sixfold alignment is arbitrary, having each orientation the same energy. In particular, in Fig. 3(d), it can be seen that there are actually two alignments present of the five available. This finding is not sensitive to the size of the simulation cell, which we have increased by a factor of 9 to confirm its validity, with and without periodic boundary conditions. The same behavior is seen during both adsorption and desorption simulation runs. In addition, during the transition at $T = 77$ K shown in Fig. 2(a), the density of fivefold defects goes from ~ 0.46 nm² (point "b") to ~ 0.26 nm² (point "c"), and this result is independent of the size of the simulation cell.

Xe adsorption on this surface was studied earlier using low-energy electron diffraction, and isobar measurements indicate that the Xe film grows layer by layer in the temperature range 65 to 80 K [17], consistent with the simulations described above. Figure 3 shows the LEED patterns obtained under similar conditions to the simulations. At the lowest coverage [Fig. 3(a)], the only discernible change in the LEED pattern from that of the clean surface is an attenuation of the substrate beams. After the adsorption of one layer [Fig. 3(b), coverage determined by the isobar measurements [17]] there are still no resolvable features that would indicate an overlayer having an order different from the substrate. At the onset of the adsorption of the second layer [Fig. 3(c)], however, the LEED pattern shows new diffraction spots that correspond to five rotational domains of a hexagonal structure. Within each of these domains, the close-packed direction of the Xe is aligned with the fivefold directions of the substrate [17], as observed in the simulation. In the experiments, all possible alignments are observed owing to the presence of all possible rotational alignments present within the width of the electron beam (0.25 mm), and there is no evidence of step-pinning of the overlayer. When the second layer is complete [Fig. 3(d)], these spots are well-defined and their widths are the same as the substrate spots, indicating a coherence length of at least 15 nm. The average Xe-Xe spacing measured in the experiment is consistent with the bulk nearest-neighbor spacing of 0.44 nm. A dynamical LEED analysis of the intensities indicates that the structure of the multilayer film is consistent with fcc Xe(111). These structure parameters for the 2-layer film are essentially identical to the results obtained for Xe growth on Ag(111) [23,24], a much weaker and less corrugated substrate. This suggests that effect of the symmetry and corrugation of the substrate potential on the Xe film structure is largely confined to the monolayer.

While the experiments are restricted to a comparatively narrow range in T and P (the LEED experiments require $P < 10^{-7}$ bar and feasible equilibration times require $P >$

10^{-13} bar) the simulations are not so restricted. Therefore, we have also investigated the adsorption of Xe at a very low temperature (20 K) and a high temperature (160 K). The density plots and FT's at the coverage corresponding to point "c" in Fig. 2 are shown on Fig. 4 for the three temperatures, 20, 77, and 160 K. The trend observed in the ordering is that the onset of sixfold ordering occurs differently at the higher temperatures. Sixfold ordering is already present at this coverage for 160 K, but is barely present at 77 K and is not present at 20 K. This trend is consistent with the substrate potential being a bigger influence on the film's structure at lower T . The development of the bulk Xe earlier at higher T may be viewed as a kind of wetting transition of the bulk Xe phase, attributable to a diminishing interfacial free energy cost with increasing T [25,26]. More thermal disorder is also evident in the film structures at higher T .

Interestingly, at all T studied, stacking faults are evident in the multilayer films. Their origin appears to be dislocations in the layers, which are most prevalent at the highest temperatures studied, as expected for entropic reasons. This is consistent with x-ray diffraction studies of the growth of Xe on Ag(111), where stacking faults were observed for Xe growth under various growth conditions [23,24], although the overall structure observed was fcc(111). Such a stacking fault is evident in Fig. 5, which shows a superposition of Xe layers 2 and 4 at point "e" in Fig. 2(a). The coincidence of the atom locations in the top left part of this figure is consistent with an hcp structure (*ABAB* stacking) whereas the offsets observed in the lower

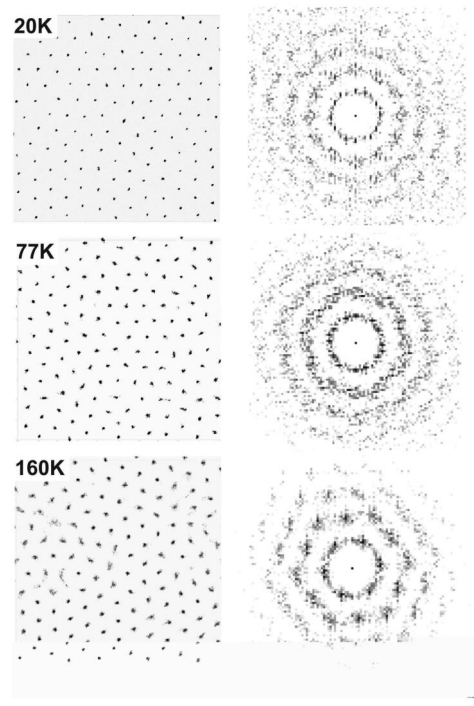


FIG. 4. Density plots and Fourier transforms for monolayer films (corresponding to point "c" in Fig. 2(a)) at 20, 77, and 160 K.

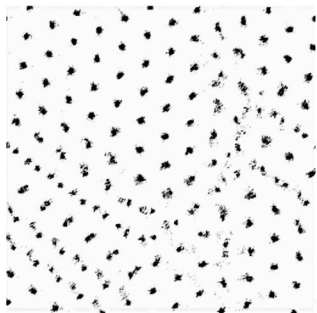


FIG. 5. Density plot corresponding to point “c” on Fig. 2(a), showing a superposition of the density slices for the 2nd and 4th layers. In the top right, 4th-layer atoms are located directly above the 2nd-layer atoms, whereas in other regions, such as lower left, the two layers are offset.

part of the figure indicate the presence of stacking faults caused by dislocations in the layers. We note that while bulk Xe has an fcc structure, and indeed an fcc structure was found for the multilayer film in the LEED study, calculations of the bulk structure using LJ pair potentials such as those employed here result in a more stable hcp structure [27]. The energy difference between the two structures is very small, and apparently arises from a neglect of d -orbital overlap interactions, which are more effective in fcc than in hcp structures [27,28]. Although the simulated film is hcp instead of fcc, the main conclusions concerning the growth mode of Xe on the quasicrystal are not affected [29].

In summary, our simulation results are consistent with the experimental data over the somewhat limited range explored thus far. A consistent pattern has emerged; the quasicrystalline order is transmitted to films of thickness less than about two layers, disappearing upon further growth of the film. The results of this study encourage confidence in the use of physical adsorption to probe film growth [29]. The extension of these calculations to the study of other properties such as lattice dynamics and friction, as well as other adsorbates, would seem well justified. Such studies will yield a comprehensive understanding of competing interactions in physisorbed layers on aperiodic substrates, as found previously on periodic surfaces.

This research was supported by NSF Grants No. DMR-0208520 and No. DMR-0505160. We wish to acknowledge helpful discussions with L. W. Bruch, J. Sofo, M. Widom, A. Kolmogorov, C. Henley, D. Rabson, and R. Trasca.

*Corresponding author.

Email address: stefano@duke.edu

- [1] E. Rotenberg, W. Theis, K. Horn, and P. Gille, *Nature (London)* **406**, 602 (2000).
- [2] E. Rotenberg, W. Theis, and K. Horn, *J. Alloys Compd.* **342**, 348 (2002).
- [3] J.M. Dubois, *Phys. Scr.* **T49A**, 17 (1993).

- [4] J.S. Ko, A.J. Gellman, T.A. Lograsso, C.J. Jenks, and P.A. Thiel, *Surf. Sci.* **423**, 243 (1999).
- [5] J.Y. Park, D.F. Ogletree, M. Salmeron, C.J. Jenks, and P.A. Thiel, *Tribol. Lett.* **17**, 629 (2004).
- [6] R. McGrath, U. Grimm, and R.D. Diehl, *Phys. World* **17**, 23 (2004).
- [7] R. McGrath, J. Ledieu, E.J. Cox, and R.D. Diehl, *J. Phys. Condens. Matter* **14**, R119 (2002).
- [8] R. McGrath, J. Ledieu, E.J. Cox, S. Haq, R.D. Diehl, C.J. Jenks, I. Fisher, A.R. Ross, and T.A. Lograsso, *J. Alloys Compd.* **342**, 432 (2002).
- [9] L.W. Bruch, M.W. Cole, and E. Zaremba, *Physical Adsorption: Forces and Phenomena* (Oxford University Press, Oxford, 1997).
- [10] J. Ledieu, J.-T. Hoelt, D.E. Reid, J. Smerdon, R.D. Diehl, T.A. Lograsso, A.R. Ross, and R. McGrath, *Phys. Rev. Lett.* **92**, 135507 (2004).
- [11] T. Cai, J. Ledieu, V. Fournée, T. Lograsso, A. Ross, R. McGrath, and P.A. Thiel, *Surf. Sci.* **526**, 115 (2003).
- [12] V. Fournée, T.C. Cai, A.R. Ross, T.A. Lograsso, J.W. Evans, and P.A. Thiel, *Phys. Rev. B* **67**, 033406 (2003).
- [13] K.J. Franke, H.R. Sharma, W. Theis, P. Gille, P. Ebert, and K.H. Rieder, *Phys. Rev. Lett.* **89**, 156104 (2002).
- [14] F. Ancilotto, S. Curtarolo, F. Toigo, and M.W. Cole, *Phys. Rev. Lett.* **87**, 206103 (2001).
- [15] S. Curtarolo, G. Stan, M.W. Cole, M.J. Bojan, and W.A. Steele, *Phys. Rev. E* **59**, 4402 (1999).
- [16] R.A. Trasca, N. Ferralis, R.D. Diehl, and M.W. Cole, *J. Phys. Condens. Matter* **16**, S2911 (2004).
- [17] N. Ferralis, R.D. Diehl, K. Pussi, M. Lindroos, I.R. Fisher, and C.J. Jenks, *Phys. Rev. B* **69**, 075410 (2004).
- [18] A similar approach was used earlier to describe the interaction of Al on quasicrystalline Al-Ni-Co; see T. Fluckiger, Y. Weisskopf, M. Erbudak, R. Luscher, and A.R. Kortan, *Nano Lett.* **3**, 1717 (2003).
- [19] N. Ferralis, K. Pussi, E.J. Cox, M. Gierer, J. Ledieu, I.R. Fisher, C.J. Jenks, M. Lindroos, R. McGrath, and R.D. Diehl, *Phys. Rev. B* **69**, 153404 (2004).
- [20] G. Vidali, G. Ihm, H.-Y. Kim, and M.W. Cole, *Surf. Sci. Rep.* **12**, 135 (1991).
- [21] A. Chizmeshya, M.W. Cole, and E. Zaremba, *J. Low Temp. Phys.* **110**, 677 (1998).
- [22] See EPAPS Document No. PRLTAO-95-067537 for the Monte Carlo simulation animation. This document can be reached via a direct link in the online article’s HTML reference section or via the EPAPS homepage (<http://www.aip.org/pubservs/epaps.html>).
- [23] P. Dai, T. Angot, S.N. Ehrlich, S.-K. Wang, and H. Taub, *Phys. Rev. Lett.* **72**, 685 (1994).
- [24] P. Dai, Z. Wu, T. Angot, S.-K. Wang, H. Taub, and S.N. Ehrlich, *Phys. Rev. B* **59**, 15464 (1999).
- [25] S. Curtarolo, G. Stan, M.J. Bojan, M.W. Cole, and W.A. Steele, *Phys. Rev. E* **61**, 1670 (2000).
- [26] S. Curtarolo, M.W. Cole, and R.D. Diehl, *Phys. Rev. B* **70**, 115403 (2004).
- [27] K.F. Niebel and J.A. Venables, in *Rare Gas Solids*, edited by M.L. Klein and J.A. Venables (Academic Press, New York, 1976), Vol. 1, p. 558.
- [28] T. Bricheno and J.A. Venables, *J. Phys. C* **9**, 4095 (1976).
- [29] W. Setyawan, N. Ferralis, R.D. Diehl, K. Pussi, M.W. Cole, and S. Curtarolo “Xe Films on a Decagonal Al-Ni-Co Quasicrystal Surface” (to be published).